

**MICROSTRUCTURE AND PHASE FORMATION IN TiC-TiB<sub>2</sub>-SiC COMPOSITES  
PROCESSED BY PULSED LASER MELTING***Robby Hermawan Yuwono, Irina Sergeevna Loginova <sup>a</sup>, Alexey Nikolaevich Solonin*

National University of Science and Technology MISIS, 4 Leninsky av., Moscow, Russia

<sup>a</sup> loginova@misis.ru**ABSTRACT**

The development of high-performance ceramic composites for extreme environments requires advanced processing techniques that can tailor microstructures and explore non-equilibrium phases. This study investigates the synthesis of TiC-TiB<sub>2</sub>-SiC composites via pulsed laser melting. The influence of powder preparation (dry planetary ball milling vs. wet mixing) and laser parameters on microstructure and phase formation was examined. Results demonstrate that dry milling for 120 minutes produced a homogeneous powder essential for consistent melting, while wet preparation led to inadequate microstructures. Laser processing above a 230 V threshold under a low-reactivity atmosphere achieved full integration of phases. Crucially, the rapid solidification triggered non-equilibrium conditions, yielding a characteristic solidification sequence and, most significantly, the formation of previously unreported peritectic ternary phases identified by EDS analysis. This work establishes pulsed laser melting as a viable route for processing TiC-TiB<sub>2</sub>-SiC composites and highlights its unique potential for discovering novel non-equilibrium microstructures in complex ceramic systems.

**KEYWORDS**

TiC-TiB<sub>2</sub>-SiC ceramic; eutectic; phase diagram; microstructure; additive manufacturing; pulse-laser melting.

**ФОРМИРОВАНИЕ МИКРОСТРУКТУРЫ И ФАЗ В КОМПОЗИТАХ TiC-TiB<sub>2</sub>-SiC,  
ПОЛУЧЕННЫХ МЕТОДОМ ИМПУЛЬСНОГО ЛАЗЕРНОГО ПЛАВЛЕНИЯ***Робби Хермаван Юовоно, Ирина Сергеевна Логинова <sup>a</sup>, Алексей Николаевич Солонин*

Университет науки и технологии МИСИС, Россия, Москва, Ленинский пр-т, 4

<sup>a</sup> loginova@misis.ru**ABSTRACT**

Разработка керамических композитов для экстремальных условий эксплуатации требует применения передовых технологических процессов, позволяющих контролировать формирование микроструктуры и неравновесных фаз. В данной работе изучен композиционный мате-

рил  $\text{TiC-TiB}_2\text{-SiC}$ , полученный методом импульсного лазерного плавления. Было исследовано влияние подготовки порошка (измельчение в среде инертного газа в планетарной шаровой мельнице и механическое перемешивание в спирте) и параметров лазерного плавления на микроструктуру и образование неравновесных фаз. Результаты показывают, что измельчение в мельнице в течении 120 минут позволило получить гомогенный порошок, необходимый для стабильного плавления, в то время как смешивание в спирте не позволяет сформировать однородную микроструктуру. Лазерная обработка при напряжении выше 230 В в атмосфере с низкой реакционной способностью обеспечила полную интеграцию фаз. Важно отметить, что быстрая кристаллизация приводит к характерной последовательности неравновесной кристаллизации и, главное, к образованию ранее не описанных перитектических тройных фаз, идентифицированных с помощью EDS-анализа. В данной работе показано, что импульсное лазерное плавление является перспективным методом обработки композитов  $\text{TiC-TiB}_2\text{-SiC}$ , и подчеркивается его уникальный потенциал для обнаружения новых неравновесных микроструктур в сложных керамических системах.

## KEYWORDS

Композит  $\text{TiC-TiB}_2\text{-SiC}$ ; эвтектика; фазовая диаграмма; микроструктура; аддитивное производство; импульсно-лазерное плавление.

## Introduction

The development of ceramic materials is driven by the needs of advanced manufacturing technology to create materials that fulfil market demands. Composite materials, which are composed of several phases, have garnered significant attention due to their tailored properties. Among the variety of composites, ceramic-based systems such as  $\text{TiC-TiB}_2\text{-SiC}$  have shown great potential in applications requiring high strength, wear resistance, and thermal stability [1, 2]. These properties are particularly important in fields like aerospace, automotive, and defense industries [3–6].

Pulsed laser melting, a subset of laser-based manufacturing techniques, has emerged as a powerful tool for processing composite materials. This method offers precise control over the resulting microstructure by manipulating parameters such as laser power, scanning speed, and beam profile [7, 8]. The technique allows for localized modification of material properties, making it an attractive option for fabricating complex geometries and customized components.

Despite progress in ceramic composite research, the study of the  $\text{TiC-TiB}_2\text{-SiC}$  eutectic

system—whether binary or ternary—remains underexplored, particularly in the context of pulsed laser melting. Preliminary studies on binary systems, such as  $\text{TiC-TiB}_2$ ,  $\text{TiB}_2\text{-SiC}$ , and  $\text{TiC-SiC}$ , have demonstrated promising results in terms of hardness, fracture toughness, and thermal stability [9–13]. However, the addition of a third component introduces complex interactions during melting and solidification, which are not yet fully understood.

This research aims to bridge this gap by investigating the influence of processing regimes on the structure and properties of  $\text{TiC-TiB}_2\text{-SiC}$  composite materials during pulsed laser melting. By establishing relationships between mechanical alloying parameters, powder particle interactions, and laser processing conditions, this study seeks to provide novel insights into the formation mechanisms and property optimization of these ceramic composites.

## 1. Materials and methods

### 1.1. Materials.

Commercial powders with different physical characteristics were used as raw materials and examined using SEM.  $\text{TiC}$  powder exhibited

high sphericity, while  $\text{TiB}_2$  and  $\text{SiC}$  powders shared an irregular shape, albeit with different sizes (as shown in fig. 1).

A composite mixture with a eutectic composition of 38 $\text{TiC}$ -27 $\text{TiB}_2$ -33 $\text{SiC}$  (wt.%) was prepared [14]. Two methods of preparation were employed, that are: wet preparation method, which 5 g of the eutectic mixture was manually mixed with 0.2–0.5 g of water until a consistent paste was achieved. The mixture was

then cast onto an aluminum strip to form a layer approximately 0.3 mm thick. The dried casts were subsequently laser melted.

The other preparation method is dry preparation; The powders were mixed using a planetary ball mill with the parameters listed in table 1. To minimize oxidation, the milling jar was purged with argon. The resulting powder mixture was then pressed at 382 MPa prior to laser melting.

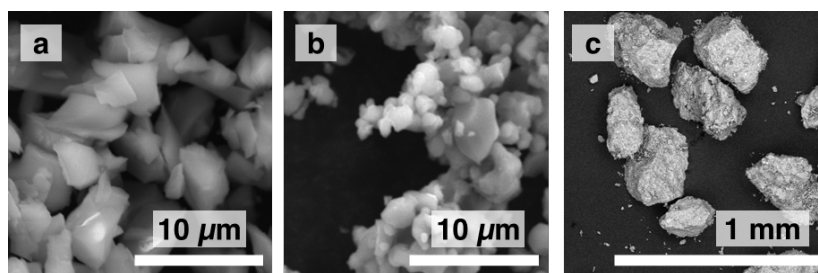


**Fig. 1.** Morphologies of (a)  $\text{SiC}$ , (b)  $\text{TiC}$ , and (c)  $\text{TiB}_2$  powders. The average particle sizes are  $4,56 \pm 1,82 \mu\text{m}$ ,  $3,07 \pm 1,35 \mu\text{m}$ , and  $317 \pm 78 \mu\text{m}$ , respectively, all with 99,5% purity

**Рис. 1.** Морфология порошков (a)  $\text{SiC}$ , (b)  $\text{TiC}$  и (c)  $\text{TiB}_2$ . Средний размер частиц составляет  $4,56 \pm 1,82 \mu\text{м}$ ,  $3,07 \pm 1,35 \mu\text{м}$  и  $317 \pm 78 \mu\text{м}$  соответственно с чистотой 99,5%

**Table 1.** Parameters of the planetary ball mill

**Таблица 1.** Параметры обработки в планетарной шаровой мельнице

Parameter	Value
Speed ratio (K) between jars and planetary wheel	2,35
Planetary wheel speed (rpm)	500
Acceleration (g)	23,8
Acceleration time (s)	20
Milling ball radiuses (mm) [1:1]	5,5 and 11
Mass of the milling balls (gr)	700
Duration of milling (mins)	15, 30, 60, 120

**Table 2.** Samples and their corresponding laser parameters

**Таблица 2.** Параметры импульсной лазерной обработки

Samples	Preparation methods	Voltage, V	Frequency, Hz	Overlap, mm
S01	Wet	200	5	0,3
S02	Dry	215	5	0,3
S03	Dry	230	10	0,1
S04	Dry	240	10	0,1
S05	Dry	250	10	0,1
S06	Dry	280	10	0,1

### 1.2. Laser melting and microstructural characterization.

The melting process was carried out using a pulsed Nd:YAG laser with a wavelength of 1064 nm. The instrument operated under a low-reactivity atmosphere. An integrated system was used to create a 2D pattern on the sample surface. Key parameters including voltage, frequency, and overlap were varied (table 2), while the pulse duration was kept constant at 12 ms for all samples. After processing, samples were mounted in a conductive mixture of epoxy and graphite to facilitate examination by scanning electron microscopy (SEM). Microstructure was first revealed using an optical microscope (OM) for initial screening, followed by detailed analysis using SEM and energy-dispersive X-ray spectroscopy (SEM-EDS, Vega3 TESCAN) to characterize morphology and chemical composition.

## 2. Results and discussion

### 2.1. Comparison between dry and wet preparation methods.

As depicted in fig. 2, a significant reduction in particle size was observed, particularly for the  $\text{TiB}_2$  particles. Compared to the initial size

of 317  $\mu\text{m}$  (fig. 1, c), the milled powders showed  $\text{TiB}_2$  particles in the range of 30–45  $\mu\text{m}$  (fig. 2). This confirms that the milling process effectively reduced particle size and narrowed the particle size distribution.

After 15 minutes of milling, no agglomerates were present. However, after 30 minutes, agglomeration occurred, forming particles up to 50  $\mu\text{m}$  in size (fig. 2, b). Fine «satellite» particles were observed on the surface of these agglomerates, which broadens the particle size distribution. The presence of both agglomerates and satellite particles results from the competing processes of particle fracturing and cold-welding during milling [15, 16].

With further milling to 60 minutes (fig. 2, c), some large particles, assumed to be  $\text{TiB}_2$ , remained. After 120 minutes (fig. 2, d), the maximum particle size was reduced to 31  $\mu\text{m}$ . Therefore, the optimal milling time was determined to be 120 minutes. Extending the milling duration beyond 30 minutes helped to prevent agglomerate formation, consistent with Bastwros's argument that the tendency for agglomeration decreases with longer milling times [17].

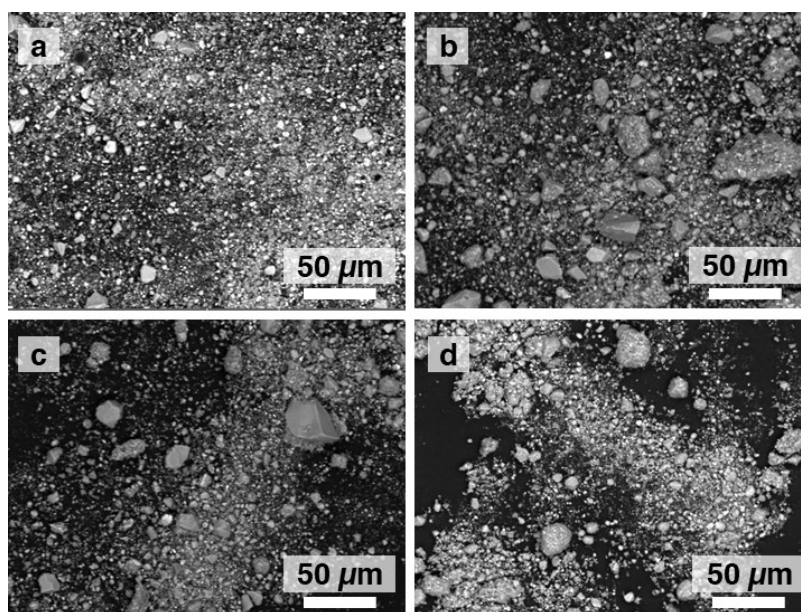


**Fig. 2.** SEM morphology of  $\text{TiC-TiB}_2\text{-SiC}$  composite powder after milling for (a) 15, (b) 30, (c) 60, and (d) 120 minutes

**Рис. 2.** Морфология композиционного порошка  $\text{TiC-TiB}_2\text{-SiC}$  после измельчения в течение (a) 15, (b) 30, (c) 60 и (d) 120 минут



From the perspective of elemental distribution, longer milling durations caused increased wear of the milling jar. While no Fe contamination was detected after 15 minutes, it appeared after 30 and 60 minutes. After the maximum milling time of 120 minutes, W contamination from the milling balls was also detected.

## 2.2. Microstructural and phase analysis.

Microstructural observations were conducted using optical microscopy (OM) for initial screening and scanning electron microscopy with energy-dispersive X-ray spectroscopy (SEM-EDS) for detailed phase and chemical analysis. While OM was ineffective for distinguishing specific compounds, SEM revealed distinct contrast: TiC appeared brightest, SiC darkest, and TiB<sub>2</sub> exhibited an intermediate gray tone. These phases displayed characteristic morphologies, with TiC grains being typically spherical [10] and TiB<sub>2</sub> forming

elongated rods [12]. Eutectic regions were identified as areas with an intimate mixture of these contrasting phases [18].

Initial analysis of the wet-prepared sample (S01, fig. 3, *a*) revealed large, unmelted grains, suspected to be TiB<sub>2</sub>. The absence of characteristic TiB<sub>2</sub> rod-like structures and the overall poor microstructure were attributed to unsteady sample formation and insufficient laser power. Consequently, the wet preparation method was discontinued in favor of the dry ball milling process.

Inspection of the dry-milled powder (fig. 3, *g*) confirmed its effectiveness, reducing the average TiB<sub>2</sub> particle size from  $317 \pm 78 \mu\text{m}$  to  $35.5 \pm 4.8 \mu\text{m}$ . This homogeneity directly translated to superior microstructures in dry-prepared samples (S02-S06, Fig. 3, *b-f*), characterized by a more uniform particle distribution and successful integration of constituents upon laser melting, as evidenced by elemental maps (fig. 4).

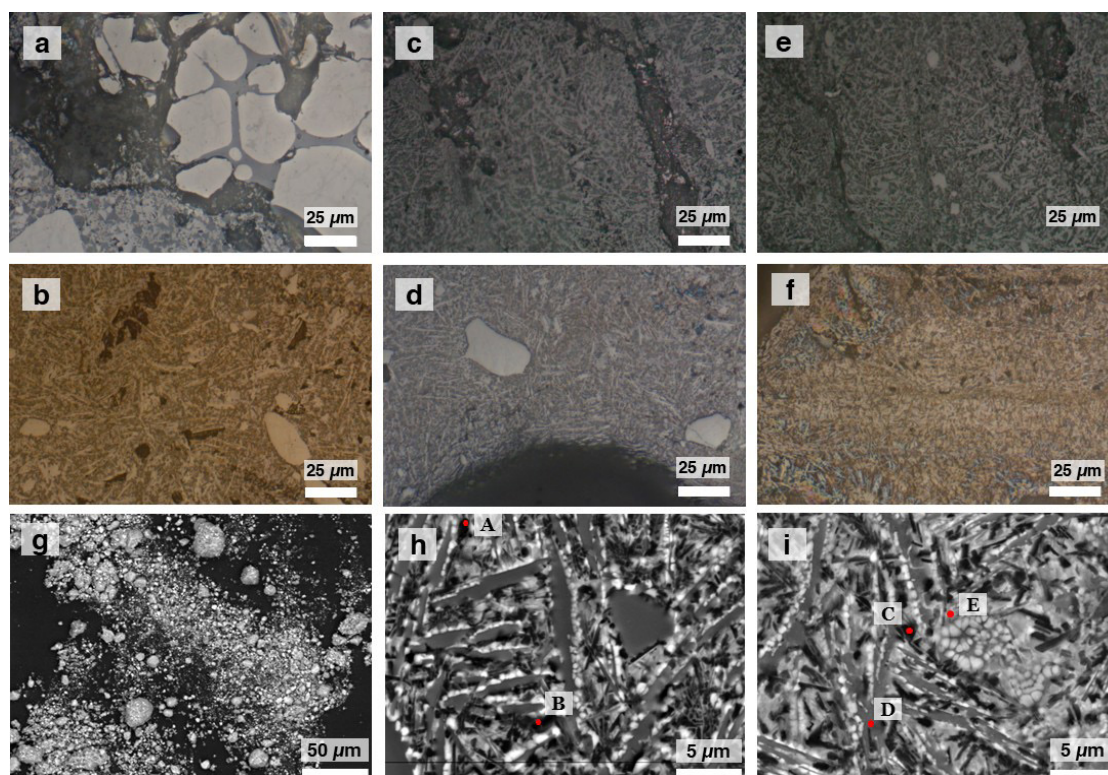


**Fig. 3.** Optical micrographs: (a) S01, (b) S02, (c) S03, (d) S04, (e) S05, (f) S06; and scanning electron micrographs: (g) milled composite powder, (h) S04, (i) S06

**Рис. 3.** Оптические изображения микроstructures: (a) S01, (b) S02, (c) S03, (d) S04, (e) S05, (f) S06; и СЭМ – изображения микроstructures (g) исходного порошка после мельницы и (h) S04, (i) S06 после лазерного плавления

The microstructures of the successfully melted samples (e.g., S04 and S07) revealed the impact of rapid solidification. Compared to prior studies conducted under slower cooling rates [12, 18, 19], the pulsed laser process triggered non-equilibrium solidification. This resulted in a distinct solidification sequence, initiating with the highest-melting-point phase ( $\text{TiB}_2$ ) and progressing to the lowest ( $\text{SiC}$ ). In sample S04 (fig. 3, *h*, fig. 4, *a*), this is observed as large primary  $\text{TiB}_2$  rods, surrounded by a layer of  $\text{TiC}$  grains, with  $\text{SiC}$  forming in the remaining interstices. The relatively large size of the  $\text{TiB}_2$  rods in S04 suggests a moderately slower local cooling rate compared to other regions.

This pattern was replicated in sample S07 (fig. 3, *i*, fig. 4, *b*), which was processed at a lower voltage, demonstrating the robustness of the dry method. Notably, while the powder composition was eutectic, the presence of primary  $\text{TiB}_2$  crystals confirms the deviation from equilibrium. This contrasts with the findings of Li et al. [19], who reported a fully eutectic microstructure with no primary phases

under their processing conditions. The difference is likely attributable to the vastly higher cooling rates in our laser melting technique, which suppress diffusion and favor primary phase formation.

Beyond the solidification sequence, elemental analysis revealed a more significant phenomenon. Contrary to literature where phases correspond strictly to  $\text{TiC}$ ,  $\text{TiB}_2$ , or  $\text{SiC}$  [3, 18], this study identified the formation of additional phases with unique compositions (table 3). While Region C approximates the binary  $\text{TiC-SiC}$  eutectic, the other regions (A, B, D, E) suggest the formation of peritectic ternary compounds not previously reported. The formation of a well-defined  $\text{TiC-SiC}$  binary eutectic is known to be challenging due to the decomposition and evaporation of  $\text{SiC}$  at high temperatures [18–20]. Furthermore, in an oxidative atmosphere, carbon from carbides can dissociate into gaseous species via diffusion of oxygen through an oxide layer [14, 21, 22], potentially contributing to the complex and non-equilibrium chemistry observed.

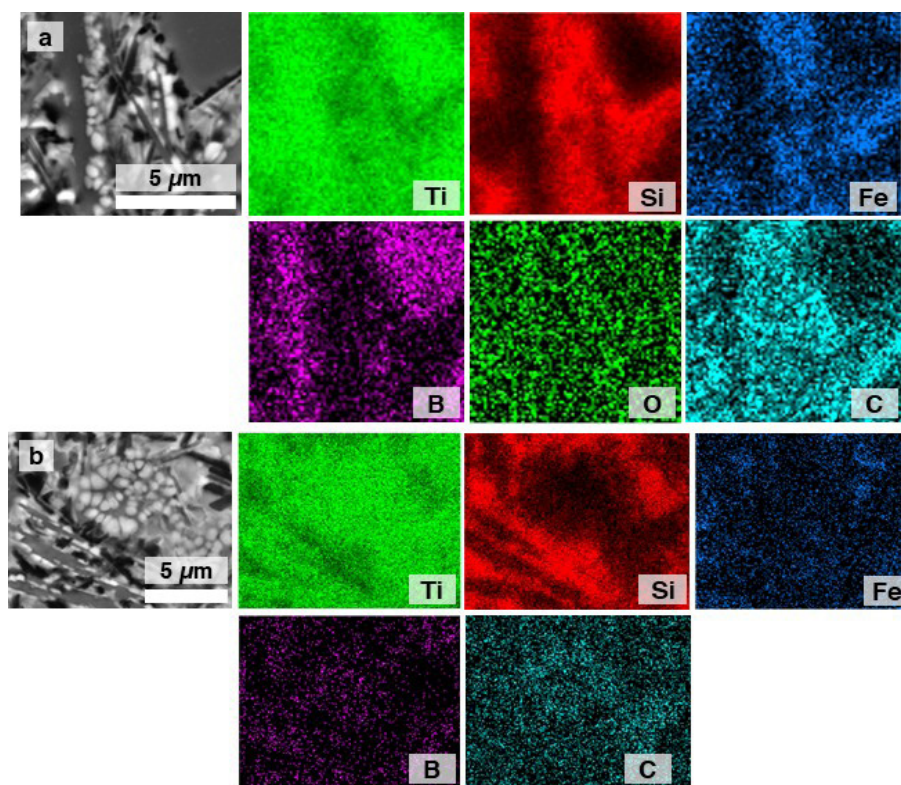


Fig. 4. Elemental distribution map of (a) S04 and (b) S06

Рис. 4. Карта распределения легирующих элементов (a) S04 и (b) S06

**Table 3.** Weight percent (wt.%) of elements in identified regions. The binary and ternary eutectic compositions are from reference [14]

**Таблица 3.** Массовая доля (%) элементов в идентифицированных областях. Бинарные и тройные эвтектические составы из источника [14]

Compound/Region	Ti	Si	B	C	Fe
TiC-TiB <sub>2</sub> -SiC (Ref.)	50.3	23.2	8.9	17.6	
TiC-SiC (Ref.)	56.0	21.0		23.0	
TiC-TiB <sub>2</sub> (Ref.)	76.6		9.4	14.0	
TiB <sub>2</sub> -SiC (Ref.)	36.9	32.5	16.7	13.9	
A	79.3	5.6	6.8	8.3	
B	70.7	18.2	4.6	4.7	1.7
C	57.6	35.1		7.3	
D	76.6	12.3	7.4	3.7	
E	86.3	5.5	2.6	5.6	

The distinctive, directionally aligned microstructures achieved by other researchers using arc-melting and floating zone methods [18, 23] highlight the influence of processing technique. While those methods excel at producing large, ordered eutectics, the present work demonstrates that pulsed laser melting offers a unique pathway to access non-equilibrium phase fields and create novel, metastable microstructures within the TiC-TiB<sub>2</sub>-SiC system.

### Conclusions

The investigation into pulsed laser melting of the TiC-TiB<sub>2</sub>-SiC system has yielded critical insights into processing parameters and revealed novel microstructural outcomes. The principal conclusions are:

- Under the non-equilibrium solidification conditions of pulsed laser melting, the formation of previously unreported peritectic ternary compounds was observed. This represents a significant finding, indicating that this technique can access metastable and non-equilibrium regions of the TiC-TiB<sub>2</sub>-SiC phase diagram, opening a pathway for developing materials with new properties.

- A clear link was established between processing parameters and microstructure. The rapid cooling rate dictated a solidification

sequence beginning with high-melting-point TiB<sub>2</sub>, followed by TiC, and finally SiC. Furthermore, a laser voltage threshold (~230 V) was identified as necessary to achieve a fully melted and integrated microstructure.

- The study established that a homogeneous, agglomerate-free powder feedstock is a prerequisite for successful laser processing. Dry planetary ball milling for 120 minutes was proven to be the optimal preparation method, producing a consistent powder that led to superior results compared to the wet method. This was further enhanced by equipment optimization, which improved energy efficiency.

In summary, this research not only establishes a viable processing framework for TiC-TiB<sub>2</sub>-SiC composites via pulsed laser melting but also highlights the technique's unique capability to produce novel, non-equilibrium microstructures. These findings contribute valuable knowledge to the field of advanced ceramic manufacturing and suggest that laser melting is a promising route for synthesizing next-generation composite materials with tailored phase compositions.

### Acknowledgments / Благодарности

*The microstructural studies were funded by the state task to MISIS University project code of FSME-2023-0005.*



*Микроструктурные исследования финансировались в рамках государственного задания, выполненного университетом МИ-СИС, код проекта FSME-2023-0005.*

## REFERENCES

1. Y. Wang, X. Y. Zheng, Y. R. Wei, and Z. W. Yang, "Microstructure evolution and mechanical properties of the TiB<sub>2</sub>-TiC-SiC composite ceramic and Nb brazed joint," *Journal of Manufacturing Processes*, vol. 92, pp. 179–188, Apr. 2023, doi: 10.1016/j.jmapro.2023.03.003.
2. B. Ren et al., "Synthesis and microwave absorption properties of TiB<sub>2</sub>-TiC(N)-SiC composite powders," *Ceramics International*, vol. 51, no. 9, pp. 12157–12166, Apr. 2025, doi: 10.1016/j.ceramint.2025.01.067.
3. S. N. Grigoriev et al., "Processing and Characterization of Spark Plasma Sintered SiC-TiB<sub>2</sub>-TiC Powders," *Materials*, vol. 15, no. 5, p. 1946, Mar. 2022, doi: 10.3390/ma15051946.
4. K. Cymerman, D. Oleszak, M. Rosinski, and A. Michalski, "Structure and mechanical properties of TiB<sub>2</sub>/TiC – Ni composites fabricated by pulse plasma sintering method," *Advanced Powder Technology*, vol. 29, no. 8, pp. 1795–1803, Aug. 2018, doi: 10.1016/j.apr.2018.04.015.
5. X. Cai, D. Wang, Y. Wang, and Z. Yang, "Microstructural evolution and mechanical properties of TiB<sub>2</sub>-TiC-SiC ceramics joint brazed using Ti-Ni composite foils," *Journal of the European Ceramic Society*, vol. 40, 2020.
6. B. AlMangour, D. Grzesiak, and J.-M. Yang, "Selective laser melting of TiB<sub>2</sub>/316L stainless steel composites: The roles of powder preparation and hot isostatic pressing post-treatment," *Powder Technology*, vol. 309, pp. 37–48, Mar. 2017, doi: 10.1016/j.powtec.2016.12.073.
7. X. Li and Y. Guan, "Theoretical fundamentals of short pulse laser-metal interaction: A review," *Nanotechnology and Precision Engineering*, vol. 3, no. 3, pp. 105–125, Sep. 2020, doi: 10.1016/j.npe.2020.08.001.
8. Z. Zhou, Z. Zhao, J. He, and R. Shi, "Pulsed Laser Polishing of Zirconia Ceramic Microcrack Generation Mechanism and Size Characterization Study," *Crystals*, vol. 14, no. 9, p. 810, Sep. 2024, doi: 10.3390/cryst14090810.
9. A. I. Gusev, "Phase Equilibria in the Ternary System Titanium–Boron–Carbon: The Sections TiCy–TiB<sub>2</sub> and B<sub>4</sub>Cy–TiB<sub>2</sub>," *Journal of Solid State Chemistry*, vol. 133, no. 1, pp. 205–210, Oct. 1997, doi: 10.1006/jssc.1997.7429.
10. D. Vallauri, I. C. Atías Adrián, and A. Chrysanthou, "TiC–TiB<sub>2</sub> composites: A review of phase relationships, processing and properties," *Journal of the European Ceramic Society*, vol. 28, no. 8, pp. 1697–1713, Jan. 2008, doi: 10.1016/j.jeurceramsoc.2007.11.011.
11. Z. Wang, H. Li, Z. Zhong, A. Yang, and Y. Wu, "Microstructure and mechanical properties of SiC joint with an in-situ formed SiC-TiB<sub>2</sub> composite interlayer," *Materials Science and Engineering: A*, vol. 735, pp. 104–113, Sep. 2018, doi: 10.1016/j.msea.2018.08.024.
12. W.-J. Li, R. Tu, and T. Goto, "Preparation of TiB<sub>2</sub>-SiC Eutectic Composite by an Arc-Melted Method and Its Characterization," *Mater. Trans.*, vol. 46, no. 11, pp. 2504–2508, 2005, doi: 10.2320/matertrans.46.2504.
13. Z. Zhu, K. Nie, P. Munroe, K. Deng, Y. Guo, and J. Han, "Synergistic effects of hybrid (SiC+TiC) nanoparticles and dynamic precipitates in the design of a high-strength magnesium matrix nanocomposite," *Materials Chemistry and Physics*, vol. 259, p. 124048, Feb. 2021, doi: 10.1016/j.matchemphys.2020.124048.
14. T. Goto and R. Tu, "Eutectic Ceramic Composites by Melt-Solidification," *J. Korean Ceram. Soc.*, vol. 56, no. 4, pp. 331–339, Jul. 2019, doi: 10.4191/kcers.2019.56.4.02.
15. J. Joy, A. Krishnamoorthy, A. Tanna, V. Kamathe, R. Nagar, and S. Srinivasan, "Recent Developments on the Synthesis of Nanocomposite Materials via Ball Milling Approach for Energy Storage Applications," *Applied Sciences*, vol. 12, p. 9312, 2022, doi: doi.org/10.3390/app12189312.
16. L. Zhang et al., "Effects of Mechanical Ball Milling Time on the Microstructure and Mechanical Properties of Mo<sub>2</sub>NiB<sub>2</sub>-Ni Cermets," *Materials (Basel)*, vol. 12, no. 12, p. 1926, 2019, doi: https://doi.org/10.3390/ma12121926.
17. M. Bastwros et al., "Effect of ball milling on graphene reinforced Al6061 composite fabricated by semi-solid sintering," *Composites Part B: Engineering*, vol. 60, pp. 118–118, 2014.
18. W.-J. Li, R. Tu, and T. Goto, "Preparation of TiC-TiB<sub>2</sub>-SiC Ternary Eutectic Composites by Arc-Melting and Their Characterizations," *Mater. Trans.*, vol. 47, no. 4, pp. 1193–1197, 2006, doi: 10.2320/matertrans.47.1193.
19. W.-J. Li, R. Tu, and T. Goto, "Preparation of directionally solidified TiB<sub>2</sub>-TiC eutectic composites by a floating zone method," *Materials Letters*, vol. 60, no. 6, pp. 839–843, Mar. 2006, doi: 10.1016/j.matlet.2005.10.028.
20. L. C. Astfalck, G. K. Kelly, X. Li, and T. B. Sercombe, "On the Breakdown of SiC during the Selective Laser Melting of Aluminum Matrix Composites," *Adv Eng Mater*, vol. 19, no. 8, p. 1600835, Aug. 2017, doi: 10.1002/adem.201600835.
21. W. Chen, R. M. White, T. Goto, and E. C. Dickey, "Directionally Solidified Boride and Carbide Eutectic



Ceramics,” J. Am. Ceram. Soc., vol. 99, no. 6, pp. 1837–1851, Jun. 2016, doi: 10.1111/jace.14287.

22. E. K. Storms, The Refractory of Carbides, vol. 2, 5 vols. in Refractory Materials, vol. 2. 1967.

23. R. Tu, W. Li, and T. Goto, “Phase Orientation of TiC-TiB<sub>2</sub>-SiC Ternary Eutectic Composite Prepared by an FZ Method,” Powder Metallurgy World Congress, pp. 859–860, 2006.